



9-*N*-Substituted berberine derivatives: Stabilization of G-quadruplex DNA and down-regulation of oncogene *c-myc*

Yan Ma, Tian-Miao Ou, Jin-Qiang Hou, Yu-Jing Lu, Jia-Heng Tan, Lian-Quan Gu, Zhi-Shu Huang*

School of Pharmaceutical Sciences, Sun Yat-Sen University, Guangzhou 510006, People's Republic of China

ARTICLE INFO

Article history:

Received 31 May 2008

Revised 11 July 2008

Accepted 12 July 2008

Available online 18 July 2008

Keywords:

9-*N*-Substituted berberine derivatives

Synthesis

c-myc G-quadruplex

Down-regulation of transcription

ABSTRACT

A series of 9-*N*-substituted berberine derivatives (**2a–j**) were synthesized and evaluated as a new class of G-quadruplex binding ligands. G-quadruplex of DNA had been proven to be the transcription controller of human *c-myc* gene. The interaction of 9-*N*-substituted berberine derivatives with G-quadruplex DNA in *c-myc* was examined via EMSA, CD spectroscopy, FRET-melting method, PCR-stop assay, competitive dialysis, cell proliferation assay and RT-PCR assay. The experiment results indicated that these derivatives could selectively induce and stabilize the formation of intramolecular parallel G-quadruplex in *c-myc*, which led to down-regulation of transcription of the *c-myc* in the HL60 lymphomas cell line. The related structure–activity relationships were also discussed.

© 2008 Elsevier Ltd. All rights reserved.

1. Introduction

The human oncogene *c-myc* plays important role in many cellular events, and the overexpression of the oncogene gene is related to the increasing of cellular proliferation in a variety of different malignant tumors, including breast, colon, cervix, small-cell lung, osteosarcomas, glioblastomas and myeloid leukemias.^{1,2} Up to 90% of the transcription of *c-myc* is controlled by the P1 and P2 promoter, and a nuclease hypersensitivity element III₁ (NHE III₁) with guanine-rich (G-rich) sequence (Fig. 1) is located at P1.^{3,4} The previous study demonstrated that the G-quadruplex presented in the promoter region of the *c-myc* functioned as a transcriptional repressor element,^{1,5–7} consequently controlling the transcription of *c-myc* via the G-quadruplex structure had emerged as an attractive target for anti-cancer therapeutic strategies (Fig. 1).

The strategy to find new chemical entities that were able to selectively interfere with *c-myc* expression by the formation/stabilization of the specific G-quadruplexes had potential applications.^{1,8} A number of G-quadruplex ligands, such as porphyrins,^{2,8,9} perylenes,⁴ had been developed and shown to induce and/or stabilize the G-quadruplex structure. The quindoline derivatives had been identified by our group to have the abilities in inducing/stabilizing the G-quadruplex structure in the NHE III₁ sequence and down-regulation of transcription of the *c-myc* in cancer cell line.^{10,11} A potential of G-quadruplex stabilizing compounds as anti-cancer agents is to refer a good case in

point for G-quadruplex stabilizing agent, quarfloxin (CX-3543), which targets ribosomal RNA biogenesis in cancer cells and is currently in clinical trials as an antitumor agent.¹²

Berberine, an alkaloid isolated from Chinese herbs, was initially used as anti-microbial agent. Berberine and its derivatives were subsequently evaluated as inhibitors of the topoisomerase I and II which were linked to anti-cancer activity.^{13–15} Recently, 13-substituted berberine derivatives were reported by Neidle's group that had the abilities to selectively bind to G-quadruplex over double-stranded DNA,¹⁶ and inhibited telomerase activity by binding

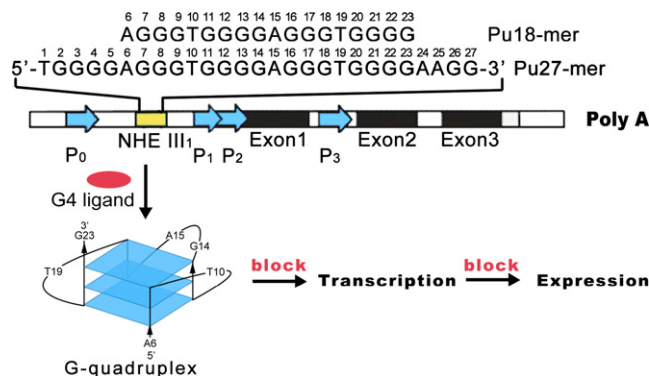


Figure 1. Location of the NHE III₁ in the *c-myc* gene and proposed biological function of G-quadruplex in this region. The numbering of the purine-rich Pu27-mer sequence and the truncated Pu18-mer are shown. When the G-quadruplex structure formed in the promoter region of *c-myc*, the transcription will be blocked.

* Corresponding authors. Tel./fax: +86 20 39332678 (L.-Q.G.); +86 20 39332679 (Z.-S.H.).

E-mail addresses: cesglq@mail.sysu.edu.cn (L.-Q. Gu), ceshzs@mail.sysu.edu.cn (Z.-S. Huang).

to G-quadruplex DNA.¹⁷ Later, our group demonstrated that 9-*O*-substituted berberine derivatives could induce and stabilize the *anti*-parallel G-quadruplex structure in the telomere DNA in the presence or absence of metal cations.¹⁸

In this work, a series of 9-*N*-substituted berberine derivatives were designed and synthesized, and the interactions between the derivatives and NHE III₁ DNA were investigated using electrophoretic mobility shift assay (EMSA), circular dichroism spectroscopy (CD), fluorescence resonance energy transfer-melting (FRET-melting) method, polymerase chain reaction-stop assay (PCR-stop assay), competition dialysis method, cell proliferation assay and reverse transcription-polymerase chain reaction (RT-PCR). All the results showed that the 9-*N*-substituted berberine derivatives could selectively stabilize the formation of intramolecular parallel G-quadruplex in *c-myc* DNA, thus led to down-regulation of the transcription of *c-myc* in cancer cell line.

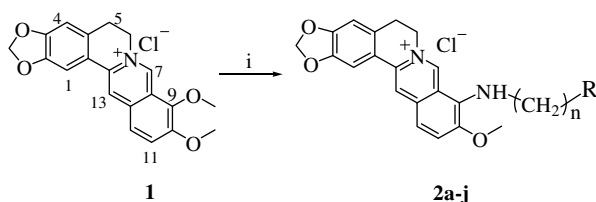
2. Results and discussion

2.1. Design and synthesis of the 9-*N*-substituted berberine derivatives

Berberine with N⁺-containing aromatic moiety (Scheme 1) appeared suitable for π - π stacking interactions with a G-quartet. In our previous studies, introduction of a side chain with terminal amino group in the 9-position of the berberine led to significant increase stabilization effect on telomeric G-quadruplex DNA and inhibitory activity on telomerase.¹⁸ It could be boiled down to the terminal amino group in the side chain strengthen the electrostatic interactions with the phosphate backbone of G-quadruplex DNA.¹⁹ Molecular modeling studies of interactions between berberine or berberine derivative **2j** and G-quadruplex structure in the NHE III₁ (A truncated sequence Pu18-mer was used for this work since nucleotides G2–G5 in the Pu27-mer not involved in the G-quadruplex structure,^{1,11} Fig. 1.) indicated that the derivatives containing 9-*N*-substituted side chain could have higher binding affinity with G-quadruplex compared to berberine, because of hydrophobic forces, electrostatic interactions, and hydrogen-bond interactions of side chain (Fig. 2). For these reasons, several 9-*N*-substituted berberine derivatives were designed and synthesized.

Compounds **2a–j** were prepared by nucleophilic aromatic displacement reaction of berberine.^{20,21} Treatment of berberine with primary amines produced amino-isoquinolinium derivatives. The synthetic route of 9-*N*-substituted berberine derivatives **2a–j** was shown in Scheme 1.

The berberine was added in a solution of anhydrous ethanol with constituent amine, and the mixture was stirred and refluxed for 2–4 h. Subsequently the mixture was concentrated and purified on Al₂O₃ column with yield of 20–51%. The yield decreased with the time prolonging. All of these compounds were characterized by NMR, ESI-MS, and element analysis.



Scheme 1. Reagents and conditions: (i) NH₂(CH₂)_nR, ethanol, reflux, 2–4 h.

2.2. Inducing G-quadruplex by 9-*N*-substituted berberine derivatives

EMSA was performed to identify whether the 9-*N*-substituted berberine derivatives induced the formation of *c-myc* G-quadruplex structures (Pu27, 5'-TGGGGAGGGTGGGGAGGGTGGGG-AAG G-3', see Fig. 1). The oligomer Pu27 was incubated with the derivatives **2a–j**, respectively, for at least 4 h in a Tris–HCl buffer (50 mM, pH 7.2).

According to the previous gel-shift data obtained under similar experimental conditions and the shift mobility of the Pu27 G-quadruplex induced by potassium ions, the major bands were identified as higher order structures (higher order) and intramolecular G-quadruplex structures (intra-G). As shown in Figure 3, all the derivatives showed interaction with the oligomer Pu27 without potassium cation. The major band was similar to the band in the presence of KCl reported previously,¹ indicated that the 9-*N*-substituted berberine derivatives might induce the formation of intramolecular G-quadruplex.

To identify the interaction of the 9-*N*-substituted berberine derivatives with *c-myc* G-quadruplex, CD spectroscopy of Pu18 was performed after treatment with berberine and its 9-*N*-substituted derivatives. The CD spectra of Pu18 without any metal cations at room temperature exhibited a small negative peak at 240 nm and a large positive peak at 275 nm. After the treatment with the 9-*N*-substituted berberine derivatives, the positive peak shifted to 262 nm and the negative peak at 240 nm was increased, which was similar with the CD spectra of Pu18 in the presence of K⁺ (Fig. 5), but no significant difference of CD spectra could be observed while equivalent berberine was added (Fig. 4A). The results indicated that the interaction abilities of the 9-*N*-substituted berberine derivatives with G-quadruplex structure were much stronger than the berberine.

The CD spectra of Pu18 titrated with **2j** in a Tris–HCl buffer was shown in Figure 4B. It could be found that the positive peak was gradually shifted from 275 nm to about 262 nm with an increase of the concentration of **2j** from 1 to 5 mol equivalences, and other derivatives exhibited the similar results with the derivative **2j**. The above results combined with the EMSA results indicated that the 9-*N*-substituted berberine derivatives could have the ability to promote the forming of G-quadruplex in the promoter region of human oncogene *c-myc*, and the G-quadruplex structures could be similar with that in the presence of K⁺.

The conformational property of the Pu18 G-quadruplex DNA induced by the 9-*N*-substituted berberine derivatives in the presence of 100 mM K⁺ and 100 mM Na⁺ was also monitored by the CD spectroscopy. As shown in Figure 5, in the presence of K⁺, Pu18 only showed a signal at about 262 nm. Upon addition berberine or **2j** to the Pu18, no significant change was appeared but the peak minor decreased. When added **2j** to Na⁺ system, the major signal shifted from 270 nm to about 262 nm, indicated **2j** could induce Pu18 to form the G-quadruplex structure like in the K⁺ system.⁷ Comparing the results in Figures 4 and 5, we could give a same

compound	n	R	compound	n	R
2a	2	N(CH ₃) ₂	2f	3	N(CH ₃) ₂
2b	2		2g	3	
2c	2		2h	3	
2d	2	OH	2i	3	
2e	2		2j	6	NH ₂

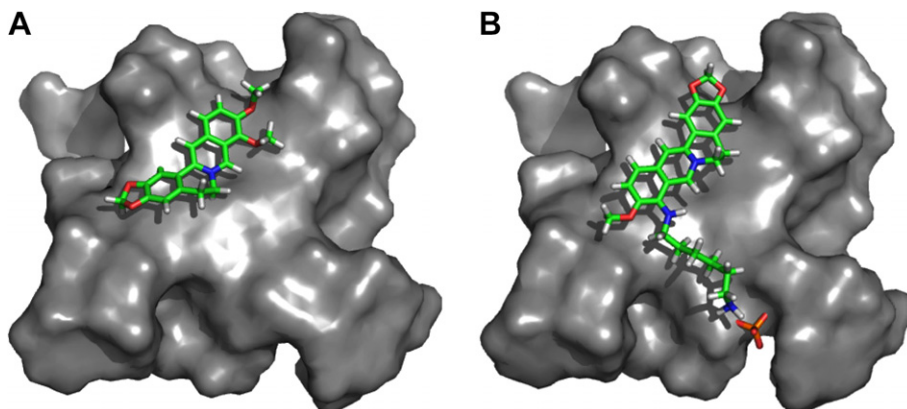


Figure 2. Models for the G-quadruplex–ligand complexes. View onto the plane of the 3' surface of Pu18B G-quadruplex.¹¹ (A) Berberine making π – π stacking interactions with the guanine tetrad. (B) 9-Substituted berberine derivative **2j** making π – π stacking interactions with G-quartet, its long side chain making hydrophobic interactions with G-quartet, and the terminal amino group in side chain making electrostatic interactions and hydrogen-bond interactions with the negative electrostatic potential phosphodiester backbone. Pictures were created with PyMOL.²²

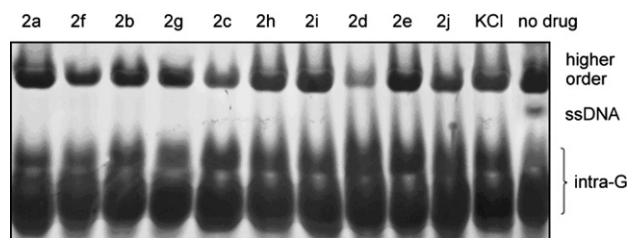


Figure 3. Polyacrylamide gel electrophoresis of the oligomer Pu27 (10 μ M) without (lane no drug) and with (left lanes) berberine derivatives **2a–j** (10 μ M), respectively. The major bands were identified as higher order structures (higher order) and intramolecular G-quadruplex structures (intra-G). KCl band: the Pu27 was incubated in the Tris–HCl buffer (pH 7.2) containing 100 mM KCl in the absence of any drugs.

conclusion that the conformational property of the Pu18 G-quadruplex in the case of **2j** was similar to that in the presence of K^+ . The results of other 9-*N*-substituted derivatives showed the similar properties.

2.3. Thermodynamic stability of the *c-myc* G-quadruplex in the presence of 9-*N*-substituted berberine derivatives

The stability of *c-myc* G-quadruplex DNA treated with the berberine and its 9-*N*-substituted derivatives were studied by FRET-melting assay. The oligomer Pu18 containing a fluorophore at the 5'-end and a fluorescence quencher at the 3'-end (FPu18T, 5'-FAM-AGGGTGGGGA-GGGTGGGG-TAMRA-3') was used in this assay. Fluorescence quenching curves were determined under different conditions with variant ion concentrations. It could be seen that the T_m values were much higher in K^+ -containing buffers than the same concentration of Na^+ -containing buffers, indicated that the G-quadruplex structure was more stable in the presence of potassium.

The melting temperature of Pu18 was monitored by FRET-melting assay in the presence of various concentrations (0.2–3.0 μ M) of 9-*N*-substituted berberine derivatives in Tris–HCl buffer containing of 0.2 mM K^+ . The results of FRET-melting assay for **2j** at different concentrations was shown in Figure 6A. It was clear that **2j** could raise the melting temperature of G-quadruplex by about 29 °C, indicated an obvious stabilization effect of **2j** on G-quadruplex in Pu18. As shown in Figure 6B, the stabilization of G-quadruplex DNA was depended on the concentration of **2j**.

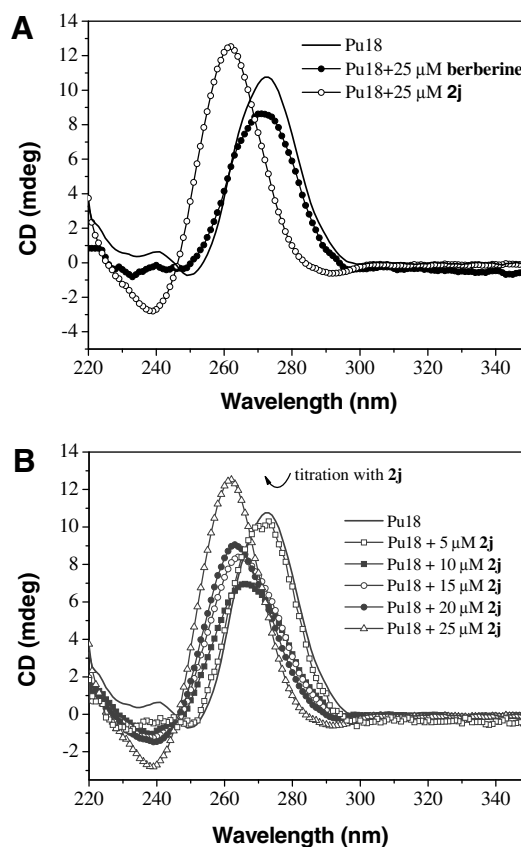


Figure 4. CD spectra of Pu18 in Tris–HCl buffer (10 mM, pH 7.2). (A) CD spectra of Pu18 in the absence of cations, the blank sample without drug was shown by solid line, the sample with 25 μ M berberine was shown by solid circle symbols (\bullet), and the sample with 25 μ M **2j** was shown by open circle symbols (\circ). (B) Change of the CD spectra of Pu18 in the presence of **2j**. The concentrations of **2j** were 0 (line), 5 (\square), 10 (\blacksquare), 15 (\circ), 20 (\bullet) and 25 (\triangle) μ M. The concentration of the Pu18 remained at 5 μ M in a Tris–HCl buffer, 10 mM, pH 7.2, in the absence of metal ions.

The T_m values of the Pu18 G-quadruplex treated with the berberine and its 9-*N*-substituted derivatives were calculated from the melting curves and listed in Table 1. The ΔT_m values of the derivatives **2a–j** were 12–29 °C, while a ΔT_m of 1.4 °C for Pu18 G-quadruplex induced by berberine indicating that the derivatives

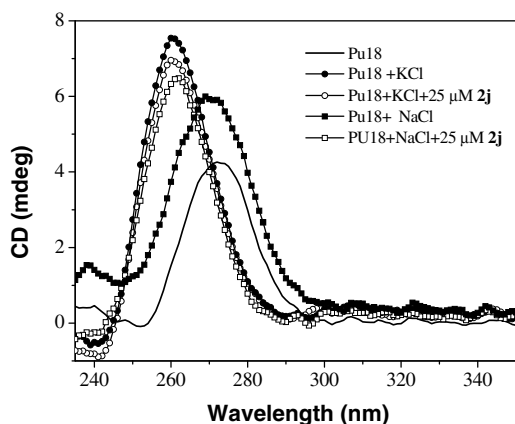


Figure 5. CD spectra of Pu18 in the presence of cations. The blank sample without drug or cations was shown by solid line, the control samples were shown by solid circle symbols (●, in the presence of K^+) and solid square symbols (■, in the presence of Na^+), and the samples with 25 μM **2j** was shown by open circle symbols (○, in the presence of K^+) and open square symbols (□, in the presence of Na^+). The concentration of the Pu18 remained at 5 μM in a Tris–HCl buffer, 10 mM, pH 7.2, in the presence of 100 mM metal ions.

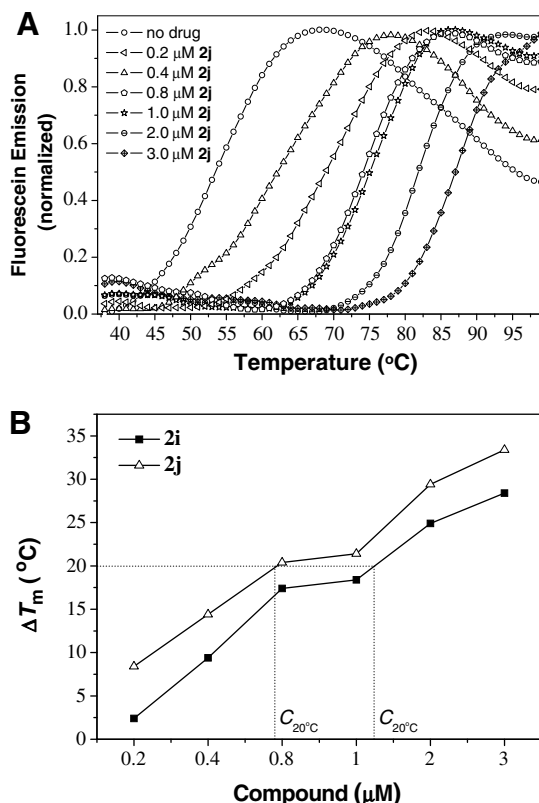


Figure 6. (A) Stabilization effects of the Pu18 in the presence of **2j** at various concentrations. (B) Concentration dependency of Pu18 stabilization (ΔT_m). Data was presented of **2i** and **2j** onto Pu18 in potassium buffer. The concentration of the Pu18 remained at 0.2 μM in a Tris–HCl buffer, 10 mM, pH 7.2, in the presence of 0.2 mM K^+ , the concentrations of **2i** and **2j** were 0.2, 0.4, 0.8, 1.0, 2.0, and 3.0 μM .

possessed a much stronger stabilizing ability to the Pu18 G-quadruplex than berberine (Fig. 7).

Furthermore, competitive FRET experiments were performed to gain further insights into their selectivity between G-quadruplex (Pu18) and duplex DNA (F10T, 5'-FAM-TATAGCTATA-HEG-TATAGC-TATA-TAMRA-3'). As shown in Table 1, the thermal stabilization of

F10T induced by the derivatives was slightly affected, indicating that the derivatives were high selective G-quadruplex binding ligands.

From the data of Table 1, **2j** had more distinct binding affinity with G-quadruplex structure than other derivatives. These results demonstrated that the structural difference in the side chains of the derivatives showed significantly different effects on the binding affinity with G-quadruplex DNA. The derivative **2j** with a 1,6-diaminoethyl side chain at the 9-position possessed higher binding affinity with G-quadruplex DNA. The derivatives with a 1,2-diaminoethyl side chain (**2a**, **2b**, and **2c**) or with a 1,3-diamino-propyl side chain (**2f**, **2g**, **2h**, and **2i**) had good binding affinity with G-quadruplex, while the derivative **2d** with a side chain containing a terminal hydroxyl group, showed a comparatively lower ΔT_m value. Interestingly, the derivative **2e** with a side chain containing a terminal phenyl group also showed a good binding affinity with G-quadruplex DNA, the ΔT_m value achieved is 20 °C.

2.4. Inhibition of amplification in the promoter region of *c-myc* by berberine derivatives

The induction of biologically relevant G-quadruplex formation in the Pu27 by the berberine derivatives was investigated using PCR-stop assay. In the presence of the derivatives, the single-strand Pu27 was folded into a G-quadruplex structure and blocked the hybridization with its complementary strand (Pu27rev). In that case, the 5' to 3' extension by the Taq polymerase was inhibited and the final double-stranded DNA product could not be detected by electrophoresis separation.

The berberine derivatives at various concentrations of 1.0, 2.5, 4.0, and 5.0 μM were used in this assay. The PCR products were separated by agarose electrophoresis and silver stained (Fig. 8). The concentrations of derivatives for inhibition of amplification by 50% (IC_{50}) were listed in Table 2. These results were correlated to the ΔT_m values in Table 1, which indicated that the stability of *c-myc* G-quadruplex induced by berberine derivatives was an important factor for inhibiting the gene amplification.

To further confirm the inhibitory effects of berberine derivatives against the stabilization of Pu27 G-quadruplex, a parallel experiment using an oligomer Pu27-13, 14 (5-TGGGGAGGGTGG AAAGGGTGGGAAGG-3) which could not form the G-quadruplex structure was performed, while no inhibition was observed under such circumstances even at the highest concentration of 5.0 μM (Fig. 8B).

2.5. Selectivity for G-quadruplex DNA and other DNA structures by berberine derivatives

To evaluate the selectivity of the berberine derivatives for G-quadruplex and other DNA structures, a competition dialysis experiment was performed using different types of DNA. Among the DNA used in the present study, the Pu18 and HTG21 could form the intramolecular G-quadruplex structures, and the HT-7 could form the intermolecular G-quadruplex structures. The HTC21 could form the i-motif structure, the $2d(T)_{21}/d(A)_{21}$ was associated to a triplex structure, the $d(T)_{21}/d(A)_{21}$ and HTG21/HTC21 were associated to a duplex structure, the $d(A)_{21}$ and $d(T)_{21}$ were single-strand purine and pyridine structures, respectively, and the HTG21mu was mutant HTG21 structure which could not form the G-quadruplex structure. Higher binding affinity was reflected by the higher concentration of bound ligands accumulated in the dialysis cassette containing the specific form of DNA.

The data in Figure 9 were shown as bar charts in which the amount of bound ligand with 10 structurally different nucleic acids was plotted. In this assay, the various nucleic acids were dialyzed simultaneously against a free ligand solution. The amount of the bound ligand was directly proportional to the binding constant

Table 1
The melting temperatures of the Pu18 or the duplex F10T treated with the berberine derivatives

Compound	T_m^a (°C)	ΔT_m^b (°C)	T_m^c (°C)	ΔT_m^d (°C)	Compound	T_m^a (°C)	ΔT_m^b (°C)	T_m^c (°C)	ΔT_m^d (°C)
None	54	0	58	—	2f	74	20	59	1
2a	73	19	58	0	2g	71	17	58	0
2b	72	18	59	1	2h	78	24	59	1
2c	74	20	58	0	2i	78	25	60	2
2d	66	12	58	0	2j	83	29	60	2
2e	74	20	59	1	Berberine	55	1	60	2

^{a,b} T_m and ΔT_m values of 0.2 μ M Pu18 incubated in the presence of KCl 0.2 mM, compound 2.0 μ M.

^{c,d} T_m and ΔT_m values of 0.2 μ M F10T incubated in the presence of KCl 0.2 mM, compound 2.0 μ M.

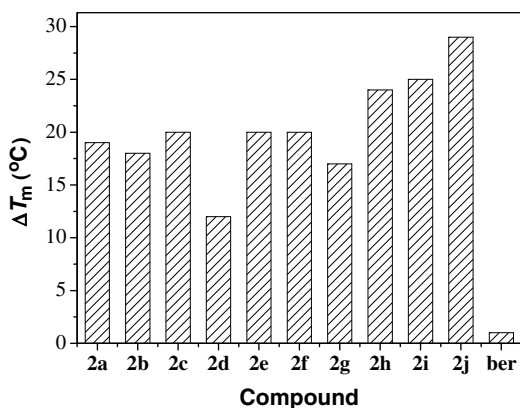


Figure 7. Stabilization of the Pu18 (0.2 μ M) treated with the derivatives at 2.0 μ M in the Tris-HCl buffer (pH 7.2) containing 0.2 mM KCl, the result was plotted as a bar graph.

for each conformer of DNA. As shown in Figure 9, the derivative **2j** binding preferentially with G-quadruplex DNA, whereas much weaker affinity for other types of DNA structures.

A high binding selectivity is an essential criterion for the use of G-quadruplex ligands in complex environments. Hence the selectivities of the derivatives for G-quadruplex DNA over double strand were evaluated again by FRET-melting assay. The T_m and ΔT_m values of the duplex F10T treated with the 9-*N*-substituted berberine derivatives were shown in Table 1. The treatment with the derivatives to duplex had a weak effect on the thermal stability of the duplex DNA ($\Delta T_m < 2$ °C) implied the derivatives were not the typical duplex DNA ligands. Compared with Pu18 FRET-melting assay

results, it was clearly that these derivatives could selectively bind to the quadruplex over duplex.

2.6. Inhibition of the transcription of *c-myc* by the berberine derivatives in the cancer cell line

To evaluate the inhibitory abilities of the derivatives on the transcription of *c-myc* in the cancer cell line, proliferation assays were carried firstly. Figure 10 showed the cell viability of HL60 lymphomas cells treated with derivative **2j** of increasing concentrations for 8 days. An inhibition of cell proliferation was found on day 2 after treatment, and a dose-dependent decrease of cell proliferation appeared after treatment with the derivative (Fig. 10). The derivative **2j** at the concentrations of 5 and 10 μ M showed a totally inhibition effect on the cell proliferation.

According to the data in above proliferation assays, the treated concentrations in the transcription assay were chosen as 0.3, 0.7, 1.7, 3.3 and 6.7 μ M to minimize the cell toxicity effect by the derivatives. For the transcription assay of *c-myc* in cancer cell lines, about 5×10^5 HL60 cells were seeded into 6-well plates and the derivative **2j** at variant concentrations were also added, and after 4-day incubation the total RNA was extracted and reverse transcribed to cDNA. The cDNA was then used as a template for specific PCR amplification of the *c-myc* sequence and controlled by β -actin.

As shown in Figure 11, the decreasing/disappearing of *c-myc* PCR products was significant when treated with derivative **2j**. The derivative **2j** at the concentrations of 0.7–1.7 μ M started to inhibit the transcription of *c-myc*, which were consistent with the PCR-stop assay results.

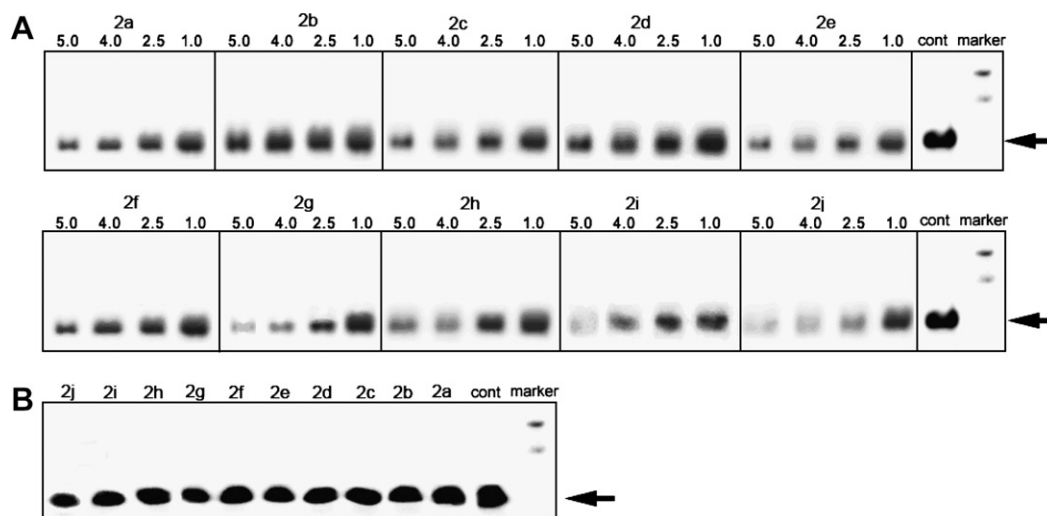


Figure 8. Effects of the berberine derivatives **2a–j** on the hybridization of the Pu27 in the PCR-stop assay. (A) 9-*N*-Substituted berberine derivatives with different concentration at 1.0 μ M, 2.5 μ M, 4.0 μ M and 5.0 μ M were added to Pu27 oligomer, as indicated according to Section 4. The band (arrow symbols) presented the 43 bp double-stranded PCR product. (B) The parallel experiments were performed using all these derivatives in oligomer Pu27-13, 14 at a concentration of 5.0 μ M.

Table 2The IC₅₀ values of berberine and its derivatives (**2a–j**) from the PCR-stop assay

Compound	2a	2b	2c	2d	2e	2f	2g	2h	2i	2j
IC ₅₀ (μM)	3.9	7.1	4.0	5.5	3.6	3.3	4.8	3.2	2.3	2.0

2.7. Cytotoxicity against tumor cells of the berberine derivatives

Table 3 showed the IC₅₀ values (cytotoxicity potency indexes) of derivatives **2a–j** against two types of tumor cells using MTT cytotoxicity assay. The berberine exhibited low or insignificant cytotoxicity to human tumor cells with the IC₅₀ values of more than 100 μM, and all the derivatives had much more potent cytotoxicity with significantly lower IC₅₀ values on tested tumor cells. Among all the derivatives, **2e** and **2j** were most potent in inhibiting the tumor cell proliferation with the lowest IC₅₀ values of 2 μM and 4 μM, respectively. As for the structure–activity relationship, the derivative **2j** bearing the longer side chains had a higher cytotoxic activity than the other derivatives. The terminal phenyl group of the derivative **2e** could participate in π–π stacking interactions with the base group and showed a higher cytotoxic activity. The cytotoxicity assay results of these derivatives were consistent with the stabilization ability of derivatives on G-quadruplex.

3. Conclusions

A new class of 9-*N*-substituted berberine derivatives (**2a–j**) were designed and semisynthesized in a convenient method. The interaction of berberine and berberine derivatives with the G-quadruplex DNA in the promoter region of the *c-myc* had been investigated in detail. Our results indicated that 9-*N*-substituted berberine derivatives could significantly induce and stabilize the parallel G-quadruplex structure formation in the presence or absence of metal cations. The derivatives with different structures had different abilities to stabilize the *c-myc* G-quadruplex. Introducing of 9-*N*-substitutes, such as a 1,6-diaminohexyl side chain, into the 9-position of berberine improves the selectivity binding with G-quadruplex and increases the inhibitory effect on the hybridization, resulting in blocking the gene expression. 9-*N*-Substituted berberine derivatives also showed obvious inhibitory effect on the transcription of *c-myc* in the cancer cell line, and higher cytotoxicity against tumor cells comparing with berberine. This study suggested that the berberine derivatives might be potential lead compounds for the development of new anti-cancer agent.

4. Experimental

¹H NMR spectra were recorded at 300 MHz on a Mercury-Plus spectrometer using TMS as an internal standard in DMSO-*d*₆ or CD₃OD/CDCl₃; MS spectra were recorded on a Shimadzu LCMS-2010A instrument with an ESI mass selective detector. Elemental analysis was carried out on an Elementar Vario EL CHNS Elemental Analyzer. Flash column chromatography was performed with silica gel (200–300 mesh) purchased from Qingdao Haiyang Chemical Co. Ltd or alumina from Sinopharm Chemical Reagent Co. Ltd. Thin-layer chromatography was carried out with Merck silica gel 60F254 glass plates.

The CD spectra were recorded on a Chirascan (Applied Photo-physics) spectrophotometer, PCR-stop assay was carried out on the Eppendorf thermocycler for DNA amplification (Mastercycler personal, 5332). FRET-melting assay was recorded on a real-time PCR apparatus (Roche Light Cycler). All oligomers/primers used in this study were purchased from Invitrogen (China), and their sequences were listed in Table 4. Acrylamide/bisacrylamide solution and *N,N,N',N'*-tetramethyl-ethylenediamine were purchased from Sigma. Taq DNA polymerase was purchased from Sangon, China. The total RNA isolation kit and the two-step RT-PCR kit were purchased from SBS Genetech, China. Stock solutions of all the derivatives (10 mM) were made using DMSO (10%) or double-distilled water. Further dilutions to working concentrations were made with double-distilled water.

Berberine chloride was isolated from Chinese herbal medicine ('Huang-Lian') and recrystallized from hot water. Compound **2a–j** were synthesized followed the procedures below.

4.1. General procedures for the preparation of **2a–j**

To a solution of berberine (0.37 g, 1 mmol) in anhydrous ethanol, the substituent amine (4–10 mmol) were added and the mixture was stirred for 2–4 h at 78 °C and the reaction was monitored by TLC. The reaction mixture was concentrated in vacuo. The residual oil was purified on Al₂O₃ column with CHCl₃/CH₃OH (100:1–30:1) as eluent to afford the proposed compound.

4.1.1. 9-*N*-2'-(*N,N*-Dimethylamino)ethylberberine (**2a**)

Berberine was treated with 2-(*N,N*-dimethylamino)ethylamine according to general procedure to give the desired product **2a** as a red solid, yield 35%. ¹H NMR (300 MHz, CDCl₃) δ: 11.18 (s, 1H), 8.47 (s, 1H), 7.54 (d, 1H, *J* = 8.6), 7.91 (s, 1H), 7.04 (d, 1H, *J* = 8.4), 6.76 (s, 1H), 6.06 (s, 2H), 5.00 (t, 2H, *J* = 6.1), 3.96 (s, 3H), 4.15 (t, 2H, *J* = 6.8), 3.31 (t, 2H, *J* = 6.1), 3.13 (t, 2H, *J* = 6.8), 2.76 (s, 6H);

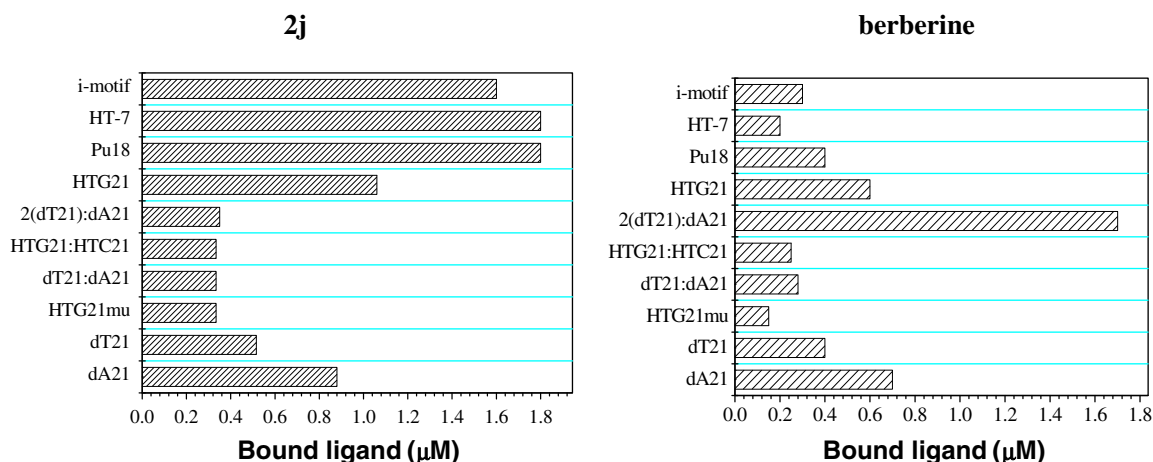


Figure 9. Results of competition dialysis experiment. One micromolar solution of **2j** or berberine was dialyzed against 10 different nucleic acid structures (45 μM) for 24 h. The amount of **2j** (left) or berberine (right) bound to each structure was plotted as a bar graph.

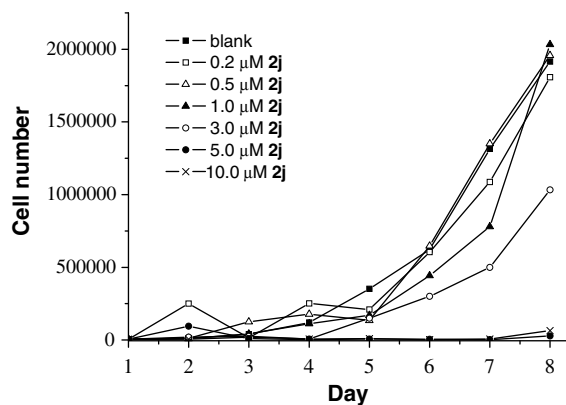


Figure 10. Effect of derivative **2j** on cell proliferation. In vitro growth curves of the HL60 lymphomas cells untreated and treated with 0 (■), 0.2 (□), 0.5 (△), 1.0 (▲), 3.0 (○), 5.0 (●) and 10.0 (×) μM of the derivative **2j**.

ESI-MS m/z : 392.55 [M–Cl]⁺. Anal. Calcd for C₂₃H₂₆N₃O₃⁺: C, 64.55; H, 6.12; N, 9.82. Found: C, 64.45; H, 6.07; N, 9.74.

4.1.2. 9-*N*-2'-(4-Morpholine)ethylberberine (**2b**)

Berberine was treated with 2-(4-morpholine)-ethylamine according to general procedure to give the desired product **2b** as a red solid, yield 45%. ¹H NMR (300 MHz, CDCl₃) δ: 11.33 (s, 1H), 7.89 (s, 1H), 7.52, 7.55 (d, 1H, $J = 8.4$), 7.28 (s, 1H), 7.13, 7.16 (d, 1H, $J = 8.4$), 6.79 (s, 1H), 6.07 (s, 2H), 5.12 (t, 2H, $J = 6.0$), 3.96 (s, 3H), 4.02 (t, 2H, $J = 6.7$), 3.70, 3.73 (t, 4H), 3.17 (t, 2H, $J = 6.0$), 2.83–2.87 (t, 2H, $J = 6.7$), 2.63 (t, 4H). ESI-MS m/z : 434.55 [M–Cl]⁺. Anal. Calcd for C₂₅H₂₈N₃O₄⁺: C, 63.89; H, 6.01; N, 8.94. Found: C, 63.80; H, 6.15; N, 8.87.

4.1.3. 9-*N*-2'-(1-Piperidine)ethylberberine (**2c**)

Berberine was treated with 2-(1-piperidine)-ethylamine according to general procedure to give the desired product **2c** as a red solid, yield 45%. ¹H NMR (300 MHz, CD₃OD/CDCl₃) δ: 10.96 (s, 1H), 7.90 (s, 1H), 7.47, 7.44 (d, 1H, $J = 8.20$), 7.09 (s, 1H), 7.17, 7.20 (d, 1H, $J = 8.20$), 6.71 (s, 1H), 6.00 (s, 2H), 5.05 (t, 2H, $J = 6.2$), 3.89 (s, 3H), 3.12 (t, 2H, $J = 6.2$), 2.69 (t, 2H), 2.44 (m, 6H), 1.51 (m, 4H), 1.39 (m, 2H); ESI-MS m/z : 432.60 [M–Cl]⁺. Anal. Calcd for C₂₆H₃₀N₃O₃⁺: C, 66.73; H, 6.46; N, 8.98. Found: C, 66.55; H, 6.35; N, 8.19.

4.1.4. 9-*N*-2'-(2-Hydroxyl)ethylberberine (**2d**)

Berberine was treated with 2-(2-hydroxyl)-ethylamine according to general procedure to give the desired product **2d** as a red

solid, yield 47%. ¹H NMR (300 MHz, DMSO-*d*₆) δ: 10.02 (s, 1H), 8.67 (s, 1H), 7.87, 7.90 (d, 1H, $J = 8.10$), 7.74 (s, 1H), 7.48, 7.51 (d, 1H, $J = 8.10$), 7.05 (s, 1H), 6.14 (s, 2H), 4.78 (t, 2H, $J = 6.0$), 3.97 (s, 3H), 3.63 (m, 4H), 3.19 (t, 2H, $J = 6.0$). ESI-MS m/z : 365.40 [M–Cl]⁺. Anal. Calcd for C₂₁H₂₁N₂O₄⁺: C, 62.92; H, 5.28; N, 6.99. Found: C, 62.87; H, 5.16; N, 6.85.

4.1.5. 9-*N*-2'-(Phenyl)ethylberberine (**2e**)

Berberine was treated with 2-phenylethylamine according to general procedure to give the desired product **2e** as a red solid, yield 51%. ¹H NMR (300 MHz, CDCl₃) δ: 11.57 (s, 1H), 7.88 (s, 1H), 7.53, 7.50 (d, 1H, $J = 8.2$), 7.30 (m, 5H), 7.16 (m, 1H), 7.14, 7.13 (d, 1H, $J = 8.2$), 6.80 (s, 1H), 6.07 (s, 2H), 5.06 (t, 2H, $J = 6.3$), 4.06 (t, 2H, $J = 7.3$), 3.92 (s, 3H), 3.40 (t, 2H, $J = 6.3$), 3.10–3.18 (t, 2H, $J = 7.3$); ¹³CNMR (300 Hz) 150.35, 148.50, 148.12, 146.57, 140.03, 139.77, 135.61, 133.43, 129.90, 129.38, 128.38, 126.09, 125.51, 120.73, 118.57, 117.60, 114.02, 108.86, 104.93, 102.29, 57.328, 54.410, 48.375, 38.187, 28.328; ESI-MS m/z : 425.45 [M–Cl]⁺. Anal. Calcd for C₂₇H₂₅N₂O₃⁺: C, 70.35; H, 5.47; N, 6.08. Found: C, 70.05; H, 5.37; N, 6.00.

4.1.6. 9-*N*-3'-(*N,N*-Dimethylamino)propylberberine (**2f**)

Berberine was treated with 3-(*N,N*-dimethylamino)propylamine according to general procedure to give the desired product **2f** as a red solid, yield 40%. ¹H NMR (300 MHz, CDCl₃) δ: 11.39 (s, 1H), 7.88 (s, 1H), 7.52 (d, 1H, $J = 8.5$), 7.28 (s, 1H), 7.14 (d, 1H, $J = 8.5$), 6.79 (s, 1H), 6.07 (s, 2H), 5.09 (t, 2H, $J = 6.1$), 3.94 (s, 3H), 3.89 (t, 2H, $J = 6.5$), 3.16 (t, 2H, $J = 6.1$), 2.63 (t, 2H, $J = 6.5$), 2.3 (s, 6H), 2.0 (m, 2H). ESI-MS m/z : 406.55 [M–Cl]⁺. Anal. Calcd for C₂₄H₂₈N₃O₃⁺: C, 65.22; H, 6.39; N, 9.51. Found: C, 65.02; H, 6.34; N, 9.42.

4.1.7. 9-*N*-3'-(4-Morpholine)propylberberine (**2g**)

Berberine was treated with 3-(4-morpholine)propylamine according to general procedure to give the desired product **2g** as a red solid, yield 37%. ¹H NMR (300 MHz, CDCl₃) δ: 11.46 (s, 1H), 7.89 (s, 1H), 7.52, 7.55 (d, 1H, $J = 8.5$), 7.28 (s, 1H), 7.14, 7.17 (d, 1H, $J = 8.5$), 6.79 (s, 1H), 6.07 (s, 2H), 5.08 (t, 2H, $J = 6.6$), 3.95 (s, 3H), 3.89 (t, 2H, $J = 6.8$), 3.81 (t, 4H), 3.16 (t, 2H, $J = 6.6$), 2.81 (t, 2H, $J = 6.8$), 2.72 (t, 4H), 2.15 (t, 2H); ESI-MS m/z : 448.60 [M–Cl]⁺. Anal. Calcd for C₂₆H₃₀N₃O₄⁺: C, 64.52; H, 6.25; N, 8.68. Found: C, 64.34; H, 6.11; N, 8.61.

4.1.8. 9-*N*-3'-(1-Piperidine)propylberberine (**2h**)

Berberine was treated with 3-(1-piperidine)propylamine according to general procedure to give the desired product **2h** as a

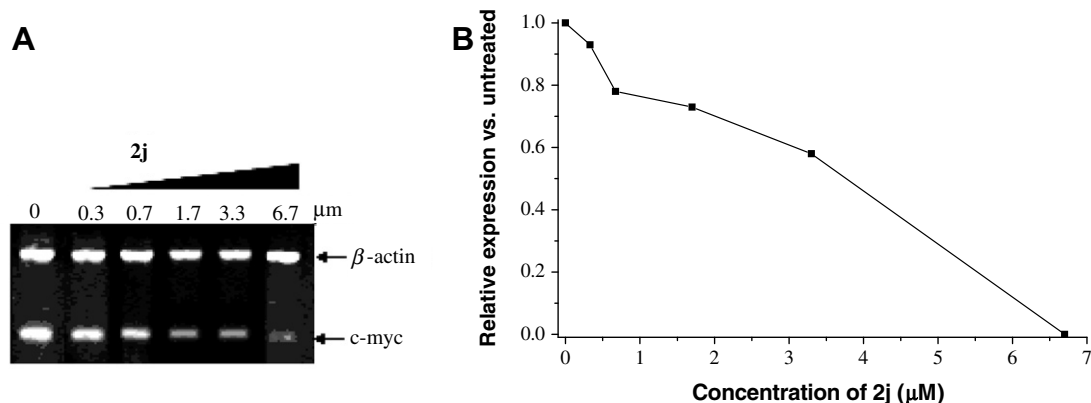


Figure 11. RT-PCR to determine the transcription of *c-myc* in the HL60 cell line treated with derivatives **2j**. (A) HL60 cells were treated with medium (no drug), 0.3, 0.7, 1.7, 3.3 and 6.7 μM of the derivative for 4 days, and the total RNA was extracted and subjected to reverse transcription, followed by PCR for *c-myc* and β -actin (control). Amplified products were 191 bp for *c-myc* and 541 bp for β -actin. (B) The optical density of each band by using Quantity One software (Biorad). The graph showed the relative expression of *c-myc* as compared with the 'no drug' sample for each time point versus concentration of the derivative.

Table 3

IC₅₀ cytotoxicity values (μM) of the berberine derivatives against tumor cells (data derived from the mean of three independent assays)

Compound	IC ₅₀ (NCl, μM)	IC ₅₀ (GLC, μM)	Compound	IC ₅₀ (NCl, μM)	IC ₅₀ (GLC, μM)
2a	36	56	2f	29	64
2b	50	50	2g	85	102
2c	22	38	2h	38	69
2d	35	51	2i	22	32
2e	2	18	2j	4	9

a red solid, yield 41%. ¹H NMR (300 MHz, CD₃OD/CDCl₃) δ: 11.34(s, 1H), 7.88 (s, 1H), 7.53, 7.51 (d, 1H, *J* = 8.5), 7.28 (s, 1H), 7.16, 7.13 (d, 1H, *J* = 8.5), 6.79 (s, 1H), 6.1 (s, 2H), 5.1 (t, 2H, *J* = 6.3), 3.94 (s, 3H), 3.91 (t, 2H, *J* = 7.2), 3.17 (t, 2H, *J* = 6.3), 2.87 (t, 2H), 2.76 (t, 2H, *J* = 7.2), 2.12 (t, 2H), 1.60 (m, 2H), 1.26 (m, 6H). ESI-MS *m/z*: 446.60 [M–Cl]⁺. Anal. Calcd for C₂₇H₃₂N₃O₃⁺: C, 67.28; H, 6.69; N, 8.72. Found: C, 67.15; H, 6.54; N, 8.62.

4.1.9. 9-*N*-3'-(1-Pyrrole)propylberberine (2i)

Berberine was treated with 3-(1-pyrrole) propylamine according to general procedure to give the desired product **2i** as a red solid, yield 43%. ¹H NMR (300 MHz, CD₃OD/CDCl₃) δ: 11.33 (s, 1H), 7.88 (s, 1H), 7.52, 7.49 (d, 1H, *J* = 8.5), 7.28 (s, 1H), 7.15, 7.11 (d, 1H, *J* = 8.5), 6.78 (s, 1H), 6.06 (s, 2H), 5.08 (t, 2H, *J* = 6.4), 3.93 (s, 3H), 3.90 (t, 2H, *J* = 6.9), 3.16 (t, 2H, *J* = 6.4), 2.84 (t, 2H, *J* = 6.9), 2.73 (t, 4H), 2.10 (t, 2H), 1.84 (m, 4H). ESI-MS *m/z*: 432.60 [M–Cl]⁺. Anal. Calcd for C₂₆H₃₀N₃O₃⁺: C, 66.73; H, 6.46; N, 8.98. Found: C, 66.65; H, 6.39; N, 8.85.

4.1.10. 9-*N*-6'-Amino hexylberberine (2j)

Berberine was treated with 1,6-hexyldiamine according to general procedure to give the desired product **2j** as a red solid, yield 43%. ¹H NMR (CD₃OD, 300 Hz) δ: 11.03 (s, 1H), 8.10 (s, 1H), 7.91 (s, 1H), 7.53 (d, 1H, *J* = 8.2), 7.16 (d, 1H, *J* = 8.2), 6.78 (s, 1H), 6.05 (s, 2H), 5.05 (t, 2H, *J* = 6.5), 3.92 (s, 3H), 3.78 (t, 2H, *J* = 6.8), 3.19 (t, 2H, *J* = 6.5), 2.93 (t, 2H, *J* = 6.8), 1.94 (s, 2H), 1.75 (m, 4H), 1.26 (m, 4H). ESI-MS *m/z*: 420.55 [M–Cl]⁺. Anal. Calcd for C₂₅H₃₀N₃O₃⁺: C, 65.85; H, 6.63; N, 9.22. Found: C, 65.35; H, 6.56; N, 9.12.

4.2. Molecular modeling

The Pu-18B G-quadruplex structure built by Tian-Miao Ou et al.¹¹ was used as the initial model to study the interaction between berberine or the berberine derivatives and human *c-myc* DNA. Ligands were constructed in SYBYL 7.3.5 (Tripos Inc., St. Louis, MO, USA). The compounds were charged using the Gasteiger-Huckel computational method. Stepwise minimizations using the Tripos force field were subsequently carried out to a convergence of 0.01 kcal mol⁻¹/Å over 5000 steps.

Table 4

Sequences of oligomers (primers) used in the present study

Oligomer	Sequence	Description
Pu27	5'-TGGGGAGGGTGGGGAGGGTGGGGAAGG-3'	Partial sequence in the promoter of oncogene <i>c-myc</i> that may form G-quadruplex
Pu27rev	5'-ATCGATCGC TTCTCGTCTCCCA-3'	Complementary sequence of Pu27 in PCR-stop assay
Pu27-13,14	5'-TGGGGAGGGTGGAAAGGGTGGGGAAGG-3'	Mutant oligomer of Pu27 that may not form G-quadruplex, whose mutant sites were 13 and 14
Pu18	5'-AGGGTGGGGAGGGTGGGG-3'	Truncated sequence of Pu27 that involved in the G-quadruplex forming
TSG4	5'-GGTTAGGGTTAGGGTTAGGG-3'	Partial sequence in human telomere that may form the G-quadruplex structure
HTC21	5'-CCTAACCCCTAACCCCTAACCC-3'	Complementary sequence of TSG4 that may form an i-motif structure
<i>c-mycA</i>	5'-TGGTGCTCCATGAGGAGACA-3'	Upstream primer for <i>c-myc</i> in RT-PCR
<i>c-mycS</i>	5'-GTGGCACCTCTTGGGACCT-3'	Downstream primer for <i>c-myc</i> in RT-PCR
<i>β-actinA</i>	5'-GTTGCTATCCAGGCTGTGC-3'	Upstream primer for <i>β-actin</i> as control in RT-PCR
<i>β-actinS</i>	5'-GCATCCTGCGCAATGC-3'	Downstream primer for <i>β-actin</i> as control in RT-PCR

Docking studies were carried out using the AUTODOCK 4.0 program.²³ Using ADT,²⁴ non-polar hydrogens of *c-myc* G-quadruplex were merged to their corresponding carbons and partial atomic charges were assigned. The non-polar hydrogens of the ligands were merged, and rotatable bonds were assigned. The resulting G-quadruplex structure was used as an input for the AUTOGRID program. The grid box was placed at the center of the G-quadruplex. The dimensions of the active site box were set at 50 × 50 × 50 Å. Docking calculations were carried out using the Lamarckian genetic algorithm (LGA). Other parameters were used default. Hundred independent docking runs were carried out for berberine and compound **2j**. Considering both the docked energy and the rmsd (root-mean-square-deviation), ligand conformation was chosen. The resulting structures were then imported into SYBYL package and minimized.

4.3. Polyacrylamide gel electrophoresis

The oligomer Pu27 at a final concentration of 10 μM was heated to 95 °C for 10 min in Tris–HCl buffer (10 mM, pH 7.2). After the solution was gradually cooled to room temperature, a 1 μL stock solution of the derivatives was added to each sample to produce the specified concentrations at a total volume of 10 μL. The reaction mixture was incubated overnight at 4 °C. After incubation, 2 μL of loading buffer (50% glycerol, 0.25% bromophenol blue, and 0.25% xylene cyanol) was added to each mixture. Ten microliter aliquots of each sample were subsequently analyzed by native 15% PAGE. The gels were silver-stained and photos were taken. The control assays were repeated as above in a Tris–HCl buffer (10 mM, pH 7.2) containing neither derivatives nor metal ion or 100 mM KCl.

4.4. CD measurements

The oligomer Pu18 at a final concentration of 5 μM was resuspended in Tris–HCl buffer (10 mM, pH 7.2) containing the derivatives to be tested. The samples were heated to 95 °C, then gradually cooled to room temperature, and incubated at 4 °C for at least 6 h. The CD spectra were recorded on Chirascan (Applied Photophysics) spectrophotometer, using 0.5 s-per-points from 220 to 450 nm and 1 nm bandwidth. The CD spectra were obtained by taking the average of two scans made from 220 to 450 nm.

4.5. FRET-melting assay

Denaturation of the oligomer FPu18T (5'-FAM-AGGGTGGG-GAGGGTGGGG-TAMRA-3'). In the experiments presented here, a real-time PCR apparatus (Roche LightCycler) was used, allowing the simultaneous recording of 32 samples. Fluorescence measurements with the Pu18 oligonucleotide (0.2 μM) were studied in the buffer (pH 7.2) containing metal ion. The melting of the G-quadruplex DNA was monitored alone or in the presence of the derivatives

Table 5
Nucleic acid conformation and samples used in competition dialysis experiments

Conformation	DNA/oligonucleotide	ϵ ($M^{-1} \text{ cm}^{-1}$)
Single-strand purine	d(A) ₂₁	255,400
Single-strand pyrimidine	d(T) ₂₁	170,700
Single strand	HTG21mu (5'-GGGTTAGAGTTAGGGTTAGGG-3')	
Duplex DNA	d(T) ₂₁ /d(A) ₂₁	12,000
Duplex DNA	HTG21/HTC21	14,800
Triplex DNA	(dT21) ₂ /d(A) ₂₁	17,200
Quadruplex DNA	Pu18 (5'-AGGGTGGGGAGGGTGGGG-3')	149,520
Quadruplex DNA	TSG4 (5'-GGGTTAGGGTTAGGGTTAGGG-3')	172,000
Quadruplex DNA	HT-7 (5'-TTAGGGT-3')	69,800
i-motif	HTC21 (5'-CCCTAACCTAACCTAACCC-3')	148,720

at 2 μM , by measuring the fluorescence of fluorescein. To test the binding selectivity of the compound to the quadruplex structure over double-stranded DNA, double-stranded DNA F10T: (5'-FAM TATAGCTATA-HEG-TATAGCTATA-TAMRA-3') was designed and measured, the melting temperature T_m is the mid-point of a melting curve at which the complex is 50% dissociated.

4.6. PCR-stop assay

The PCR-stop assay was performed with a modified protocol of the previous study.⁸ Sequences of the test oligomers, including Pu27, Pu27-13,14, and the corresponding complementary sequence used in the current study were presented in Table 4. The reactions were performed in 1 \times PCR buffer, containing 10 μmol of each pair of oligomers, 0.16 mM dNTP, 2.5 U Taq polymerase, and the indicated amount of the derivatives in Figure 8. Reaction mixtures were incubated in a thermocycler, with the following cycling conditions: 94 $^\circ\text{C}$ for 3 min, followed by 30 cycles of 94 $^\circ\text{C}$ for 30 s, 58 $^\circ\text{C}$ for 30 s, and 72 $^\circ\text{C}$ for 30 s. Amplified products were resolved on 15% nondenaturing polyacrylamide gels in 1 \times TBE and silver stained.

4.7. Competition dialysis

A Tris-HCl buffer (10 mM, pH 7.2) containing 100 mM NaCl was used for all experiments. For each competition dialysis assay, 300 mL of dialysate solution containing the derivative **2j** or berberine or **2i** at 1 μM was placed into a beaker. A volume of 500 μL at 45 μM monomeric unit (single strands, double strands, i-motif, triplet or quartet) of each of the nucleic acids samples was pipetted into a separate 0.5 mL DispoDialyzer[®] (Spectrum Laboratories, Inc.). A panel of 10 different nucleic acid structures used was listed in Table 5. All the 10 dialysis units were then placed in the beaker containing dialysate solution (Tris-HCl containing 1 μM derivative). The contents were allowed to equilibrate with continuous stirring for 24 h at room temperature. At the end of the equilibration period, DNA samples were carefully removed to microfuge tubes, and treated with 1% SDS. The ligand concentration in each sample was determined by UV absorbance.

4.8. Cell culture

The human lymphomas cell line HL60 was purchased from the Center of Experiment Animal of Sun Yat-sen University. The cells cultures were maintained in RPMI-1640 medium supplemented with 10% fetal bovine serum, 100 U/mL penicillin, and 100 $\mu\text{g}/\text{mL}$ streptomycin in 25 cm^2 culture flasks at 37 $^\circ\text{C}$ humidified atmosphere with 5% CO_2 .

4.9. Proliferation assay

For the proliferation assay, about 5000 HL60 cells were seeded in a 24-well microplate, and the freshly dissolved derivative **2j** at

increasing concentrations ranging from 0 μM to 10 μM were added to the culture medium, which were then left for 4 days. Then, at day 5, the compounds were re-added to medium and left for an additional 4 days. Cell counts and viability (Trypan blue dye exclusion) were determined daily, from day 1 to day 8 of culture. The compounds dose inhibition cell proliferations by 50% (IC_{50}) were calculated at 8 day of treatment.

4.10. RNA extraction

For RNA extraction, about 5×10^5 HL60 cells were seeded in 6-well plates, and the freshly dissolved derivative **2j** at increasing concentrations were added into the plates After 4-day cultured, the cell pellets were lysed in TRIzol solution and the total RNA was extracted according to the protocol and eluted in distilled, deionized water with 0.1% diethyl pyrocarbonate (DEPC) to a final volume of 50 μL . RNA was quantitated spectrophotometrically and stored at -80°C .

4.11. RT-PCR

Total RNA was used as a template for reverse transcription using the following protocol: each 20 μL reaction contained 1 \times M-MLV buffer, 500 μM dNTP, 100 pmol oligo dT primer, 100 U of M-MLV reverse transcriptase, DEPC in water (DEPC-H₂O), and 1 μg of total RNA. Mixtures were incubated at 42 $^\circ\text{C}$ for 60 min for reverse transcription and then at 92 $^\circ\text{C}$ for 10 min to inactivate the enzyme. PCR was performed according to the following protocol: each 20 μL reaction contained 1 \times PCR buffer, 500 μM dNTPs, 0.15 μM β -actin primers, 1.5 μM *c-myc* primers, 1 U of Taq polymerase, 0.1% DEPC-H₂O, and 3 μL of the cDNA template. The reactions were incubated in a Thermal Cycler as follows: 95 $^\circ\text{C}$ for 5 min, followed by 36 cycles of 95 $^\circ\text{C}$ for 1 min, 50 $^\circ\text{C}$ for 1 min, and 72 $^\circ\text{C}$ for 1 min. The amplified products were separated on a 1.5% agarose gel, and photos were taken on a Gel Doc 2000 Imager System.

Acknowledgements

We thank the Natural Science Foundation of China (20772159), the NSFC/RGC Joint Research Scheme (Grant 30731160006), the Science Foundation of Guangzhou (2006Z2-E402), the Science Foundation of Zhuhai (Grant PC20041131), and the NCET for financial support of this study.

References and Notes

- Siddiqui-Jain, A.; Grand, C. L.; Bearss, D. J.; Hurley, L. H. *Proc. Natl. Acad. Sci. U.S.A.* **2002**, *99*, 11593.
- Seenisamy, J.; Bashyam, S.; Gokhale, V.; Vankayalapati, H.; Sun, D.; Siddiqui-Jain, A.; Streiner, N.; Shinya, K.; White, E.; Wilson, W. D.; Hurley, L. H. *J. Am. Chem. Soc.* **2005**, *127*, 2944.
- Simonsson, T.; Pecinka, P.; Kubista, M. *Nucleic Acids Res.* **1998**, *26*, 1167.
- Rangan, A.; Fedoroff, O. Y.; Hurley, L. H. *J. Biol. Chem.* **2001**, *276*, 4640.

5. Freyer Matthew, W.; Buscaglia, R.; Kaplan, K.; Cashman, D.; Hurley Laurence, H.; Lewis Edwin, A. *Biophys. J.* **2007**, *92*, 2007.
6. Maiti, S.; Chaudhury, N. K.; Chowdhury, S. *Biochem. Biophys. Res. Commun.* **2003**, *310*, 505.
7. Seenisamy, J.; Rezler, E. M.; Powell, T. J.; Tye, D.; Gokhale, V.; Joshi, C. S.; Siddiqui-Jain, A.; Hurley, L. H. *J. Am. Chem. Soc.* **2004**, *126*, 8702.
8. Lemarteleur, T.; Gomez, D.; Paterski, R.; Mandine, E.; Mailliet, P.; Riou, J.-F. *Biochem. Biophys. Res. Commun.* **2004**, *323*, 802.
9. Grand, C. L.; Han, H.; Munoz, R. M.; Weitman, S.; Von Hoff, D. D.; Hurley, L. H.; Bearss, D. J. *Mol. Cancer Ther.* **2002**, *1*, 565.
10. Zhou, J.-L.; Lu, Y.-J.; Ou, T.-M.; Zhou, J.-M.; Huang, Z.-S.; Zhu, X.-F.; Du, C.-J.; Bu, X.-Z.; Ma, L.; Gu, L.-Q.; Li, Y.-M.; Chan, A. S.-C. *J. Med. Chem.* **2005**, *48*, 7315.
11. Ou, T.-M.; Lu, Y.-J.; Zhang, C.; Huang, Z.-S.; Wang, X.-D.; Tan, J.-H.; Chen, Y.; Ma, D.-L.; Wong, K.-Y.; Tang, J. C.-O.; Chan, A. S.-C.; Gu, L.-Q. *J. Med. Chem.* **2007**, *50*, 1465.
12. Bates, P.; Mergny, J. L.; Yang, D. *EMBO Rep.* **2007**, *8*, 1003.
13. Qin, Y.; Pang, J. Y.; Chen, W. H.; Zhao, Z. Z.; Liu, L.; Jiang, Z. H. *Chem. Biodivers.* **2007**, *4*, 481.
14. Kim, S. A.; Kwon, Y.; Kim, J. H.; Muller, M. T.; Chung, I. K. *Biochemistry* **1998**, *37*, 16316.
15. Kang, M. R.; Chung, I. K. *Mol. Pharmacol.* **2002**, *61*, 879.
16. Gornall, K. C.; Samosorn, S.; Talib, J.; Bremner, J. B.; Beck, J. L. *Rapid Commun. Mass Spectrom.* **2007**, *21*, 1759.
17. Franceschin, M.; Rossetti, L.; D'Ambrosio, A.; Schirripa, S.; Bianco, A.; Ortaggi, G.; Savino, M.; Schultes, C.; Neidle, S. *Bioorg. Med. Chem. Lett.* **2006**, *16*, 1707.
18. Zhang, W.-J.; Ou, T.-M.; Lu, Y.-J.; Huang, Y.-Y.; Wu, W.-B.; Huang, Z.-S.; Zhou, J.-L.; Wong, K.-Y.; Gu, L.-Q. *Bioorg. Med. Chem.* **2007**, *15*, 5493.
19. Harrison, R. J.; Cuesta, J.; Chessari, G.; Read, M. A.; Basra, S. K.; Reszka, A. P.; Morrell, J.; Gowan, S. M.; Incles, C. M.; Tanius, F. A.; Wilson, W. D.; Kelland, L. R.; Neidle, S. *J. Med. Chem.* **2003**, *46*, 4463.
20. Naruto, S.; Mizuta, H.; Nishimura, H. *Tetrahedron Lett.* **1976**, *17*, 1597.
21. Hassner, A.; Munger, P.; Belinka, B. A. *Tetrahedron Lett.* **1982**, *23*, 699.
22. DeLano, W. L. *The PyMOL Molecular Graphics System*; DeLano Scientific: San Carlos, CA, 2002.
23. Morris, G. M.; Goodsell, D. S.; Halliday, R. S.; Huey, R.; Hart, W. E.; Belew, R. K.; Olson, A. J. *J. Comput. Chem.* **1998**, *19*, 1639.
24. Sanner, M. F. *J. Mol. Graphics Modell.* **1999**, *17*, 57.